

Article

The Relationship between Changes in Hydro-Climate Factors and Maize Crop Production in the Equatorial African Region from 1980 to 2021

Isaac Kwesi Nooni ¹, Faustin Katchele Ogou ², Daniel Fiifi Tawiah Hagan ³, Abdoul Aziz Saidou Chaibou ⁴, Nana Agyemang Prempeh ⁵, Francis Mawuli Nakoty ⁶, Zhongfang Jin ⁷ and Jiao Lu ^{1,*}

¹ School of Atmospheric Science and Remote Sensing, Wuxi University, Wuxi 214105, China; nooni25593@alumni.itc.nl

² Laboratory of Atmospheric Physics, Department of Physics, University of Abomey-Calavi, Cotonou 01 BP 526, Benin; ogofaustin@gmail.com

³ Hydro-Climate Extremes Lab, Ghent University, 9000 Ghent, Belgium; daniel.hagan@ugent.be

⁴ Département de Physique, Faculté des Sciences et Techniques, Université Abdou Moumouni, Niamey BP 10662, Niger; abdoulaziz.saidou@uam.edu.ne

⁵ School of Geosciences, Department of Atmospheric and Climate Science, University of Energy and Natural Resources, Sunyani P.O. Box 214, Ghana; agyemang.prempeh@uenr.edu.gh

⁶ School of Electronic and Information Engineering, Nanjing University of Information Science and Technology, Nanjing 210044, China; francisnakoty@outlook.com

⁷ School of Electronic and Information Engineering, Wuxi University, Wuxi 214105, China; jinzhongfang@cw Xu.edu.cn

* Correspondence: jiao_lu@cw Xu.edu.cn

Abstract: Agricultural production across the African continent is subjected to various effects of climate variability. One of the main staple foods in Sub-Saharan Africa is maize. However, limited scientific research has recently focused on understanding the possible effects of hydro-climatic variability on maize production. The aim of the present work was to contribute to policy and climate adaptation, thus reducing the vulnerability of maize production to climate change over Equatorial Africa. This study firstly examined long-term trends of precipitation (PRE), soil moisture (SM), actual evapotranspiration (E), and potential evapotranspiration (Ep), as well as surface air temperatures, including the minimum (TMIN) and maximum (TMAX). Secondly, the relationship between maize production and these climate variables was quantified for 18 Equatorial African countries (EQCs) over 1980–2021. To assess the linear trends, Mann–Kendall and Sen’s slope tests were used to quantify the magnitude of the hydro-climatic variable trends at the 5% significance level, and Pearson’s correlation coefficient was used to evaluate the relation of these climate parameters with the maize production. The annual mean PRE declined at $0.03 \text{ mm day}^{-1}10\text{a}^{-1}$. Other climate variables increased at different rates: SM at $0.02 \text{ mm day}^{-1}10\text{a}^{-1}$, E at $0.03 \text{ mm day}^{-1}10\text{a}^{-1}$, Ep at $0.02 \text{ mm day}^{-1}10\text{a}^{-1}$, TMIN and TMAX at $0.01 \text{ }^{\circ}\text{C day}^{-1}10\text{a}^{-1}$. A regional analysis revealed heterogeneous significant wet–dry and warm–cool trends over the EQCs. While, spatially, dry and warm climates were observed in the central to eastern areas, wet and warm conditions dominated the western regions. Generally, the correlations of maize production with the E, Ep, TMAX, and TMIN were strong ($r > 0.7$) and positive, while moderate ($r > 0.45$) correlations of maize production with PRE and SM were obvious. These country-wide analyses highlight the significance of climate change policies and offer a scientific basis for designing tailored adaptation strategies in rainfed agricultural regions.

Keywords: climatology; precipitation; temperature; evapotranspiration; soil moisture; maize production; yield; climate change; Equatorial Africa



Citation: Nooni, I.K.; Ogou, F.K.; Hagan, D.F.T.; Saidou Chaibou, A.A.; Prempeh, N.A.; Nakoty, F.M.; Jin, Z.; Lu, J. The Relationship between Changes in Hydro-Climate Factors and Maize Crop Production in the Equatorial African Region from 1980 to 2021. *Atmosphere* **2024**, *15*, 542. <https://doi.org/10.3390/atmos15050542>

Academic Editor: Hanbo Yang

Received: 30 March 2024

Revised: 21 April 2024

Accepted: 26 April 2024

Published: 28 April 2024



Copyright: © 2024 by the authors. Licensee MDPI, Basel, Switzerland. This article is an open access article distributed under the terms and conditions of the Creative Commons Attribution (CC BY) license (<https://creativecommons.org/licenses/by/4.0/>).

1. Introduction

The rising global average temperature and changing precipitation regimes are expected to alter moisture conditions in various global land regions [1]. However, there are

currently numerous differences between such changes in different global regions—with either positive, negative, or stationary trends in the moisture conditions [1,2]. Changes in moisture conditions widely affect the agricultural sector [3,4]. Simultaneously, increasing food supplies to meet the demands of the growing population has been of great concern, as climate change poses significant threats to sustainable food production [1,2,5]. Moreover, countries in sub-Saharan Africa (SSA) are vulnerable to climate change threats as 70% of their economy relies heavily on agriculture [6–8]. Crop production in many SSA countries is mainly rainfed and carried out by small-holder farmers who lack adequate resources [6,9,10]. In SSA, cereal crops are predominantly grown on a subsistence basis to meet nutritional needs [11]. The maize crop represents the majority of the dietary or nutritional components of food in SSA, highlighting its high use [6–8,11–13]. According to the Food and Agriculture Organization [FAO], maize (*Zea mays* L.) is among the most widely cultivated cereal crops and a major dietary component in food [12,14]. However, in a warming climate, maize yields are affected by drought or flood events [4,15–17], which has been documented across different global land areas [14,15,18] using crop models [19], regional climate scenarios based on simulation data [20,21], and statistical methods based on historical data [22].

From a statistical perspective, the relationships between crop yield or production and climate variables (mainly precipitation and temperature) have been documented. In SSA countries, due to data availability, precipitation deficits and temperature anomalies are often used to quantify the roles of climate variables in explaining changes in crop yields [22–24]. Furthermore, many studies have focused on single national- or country-level analyses [22,25], but there are little transboundary or regional studies [7]. Maize production is influenced by moisture conditions (as a limiting factor for plant growth under certain temperature conditions) [4,15]. However, as gridded datasets are available from various sources (e.g., gauges, reanalyses, and satellites), we can assess how other climate variables such as atmospheric water demand (i.e., evapotranspiration) [26] and soil moisture availability to plants (soil moisture) [27] influence maize growth in certain regions. Assessing the trends and seasonality of several climate variables has gained attention [28,29]. For example, previous studies have deduced the trends and seasonality of several climate parameters in transboundary research on SSA [29], West Africa [28], and East Africa [30], but there are still differences in the reported trend dynamics due to the different spans of study areas and data periods used [31]. The impact of climate change on maize production or yields has also not been comprehensively studied across SSA [7,21]. The few studies on the impacts of climate change on crop production or yield (i.e., focusing on precipitation and temperature variables) were limited to single-country analyses [22,32–34]. Since climate variables have different dynamics, their impact is still uncertain considering that, to date, not many national statistical analyses have been conducted on climate dynamics and crop production in the Equatorial Africa region, where food insecurity still persists [8]. There are still gaps in the research on the impact of climate variability on maize production in the Equatorial Africa region. This study not only includes a trend analysis, as analyzed in previous studies, but we also analyzed the dynamics of six climate variables in 18 countries, which was previously unexplored in past studies. In addition, this study provides analyses on the responses to climate seasonality and trends in these six climate variables. It was necessary to conduct an in-depth investigation into the impacts of climate trends and dynamics on maize production for multiple countries in the Equatorial Africa region. To the best of our knowledge, this study presents the first multiple-country analysis of these six (6) climate variables based on the annual data and growing seasons of maize production in 18 countries in this region. Thus, the aim of this paper was to identify significant trends in multiple climate variables and their association with maize production in Equatorial African countries. The study objectives were as follows: (1) to investigate the annual and inter-annual variability and trends of precipitation, soil moisture, actual and potential evapotranspiration, and air surface temperatures (minimum and maximum) from 1980 to 2021; (2) to evaluate maize production and climate trends in 18 selected Equatorial African

countries (EQCs); and (3) to determine the relationships between these climatic variables and maize production.

The remainder of this paper is structured as follows: Section 2 introduces the study area, data sources, and methods used in this study. Section 3 presents the study results. Section 4 discusses the results of the study. Section 5 concludes the research work.

2. Materials and Methods

2.1. Study Area

The Equatorial Africa region is located in the tropics and this study focused on regions at a longitude of 18 °W–55 °E and latitude of 2 °N–20 °N. The study area (Figure 1a) is divided into 8 major climatic zones, namely semi-arid, arid, and humid zones (see Figure 1b). The study area shows that lowlands are distributed in the western regions and mountains are located in the eastern region (Figure 1c). The region is dominated by oceanic (Atlantic and Indian Oceans) and remote (teleconnections) influences [35]. The terrain of the study area ranges from –380 to 5885 m above sea level, and the highest altitude of 5800 m above sea level is in the Ethiopian Highlands (Figure 1c). The dominant vegetation types in the region are forests, grasses, shrubs, and crops (Figure 1d). The cereal crops grown in this tropical African region are mainly interspersed in dominant vegetations such as forests, grasses, and shrubs [36] (Figure 1d). All of these complex regional features, together with other climate features, define the region’s distribution of rainfall and temperatures, which influences agricultural crop production [28,37].

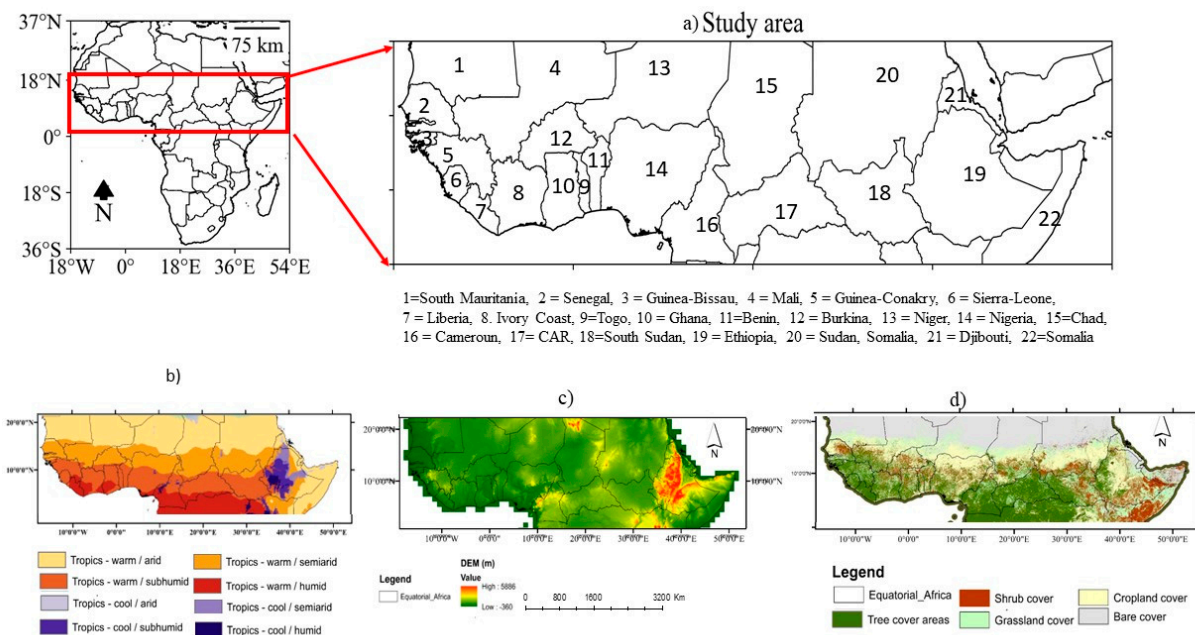


Figure 1. Spatial distribution of (a) Equatorial African countries (EQCs), (b) the Köppen climate classification [38], (c) elevation [39], and (d) land use/land cover (LULC) [40].

2.2. Data Sources

2.2.1. Climate Datasets

We used the National Oceanic and Atmospheric Administration (NOAA) Climate Prediction Center (CPC) Global Unified Gauge-Based Analysis of Daily Precipitation and Temperature for this study [41]. The CPC Unified_v1. 0/TD dataset is a high-resolution gauge-based gridded dataset developed by the NOAA CPC with a spatial resolution of 0.5° by 0.5° that includes monthly timestep data on climate variables [42].

This dataset is publicly available and was downloaded from the NOAA portal [43].

We also obtained the following satellite-based datasets. The Global Land Evaporation Amsterdam Model (GLEAM) provides satellite-based data available from 1980 to 2021,

with a high resolution of $0.25^\circ \times 0.25^\circ$. Daily scales for the surface soil moisture and actual and potential evapotranspiration were obtained from datasets on the GLEAM website [44]. For detailed information on the GLEAM datasets, readers are directed to the following references: [45–47].

2.2.2. Maize Crop-Based Data

Country-level data on maize statistics were obtained from the US Department of Agriculture (USDA) website [48]. We obtained data on the maize production and harvested area for countries in the EQA region (Table 1), with time-series data from 1950 to the present.

Table 1. List of selected countries in the Equatorial Africa region.

Number	Countries
1	South Mauritania
2	Senegal
3	Guinea-Bissau
4	Mali
5	Guinea Conakry
6	Sierra Leone
7	Liberia
8	Ivory Coast
9	Togo
10	Ghana
11	Ivory Coast
12	Burkina Faso
13	** Niger
14	Nigeria
15	Chad
16	Cameroon
17	Central African Republic (CAR)
18	** South Sudan
19	Ethiopia
20	Sudan
21	** Djibouti
22	Somalia

** denotes countries that were not included in the study due to data availability.

The period of data used for statistical analysis was from 1980 to 2021. The climate data analyses were performed using Climate Data Operators (CDO) version 1.9cl [49]. In addition, daily data were converted into annual values to match the maize crop data.

2.3. Methods

2.3.1. Maize Yield Computation

We computed the maize yields as an average ratio of production (1000 MT) per harvested area (1000 MHa). A limitation of this approach to computing yield is that it does not reflect the years in which maize production losses occurred. We computed the correlation at the country level and across the EQA region.

$$Y_{ij} = \frac{\text{Production}}{\text{Harvested}} \quad (1)$$

2.3.2. Index Anomalies

All datasets were standardized using the standardized anomalies formula (Equation (1)) based on the 1983–2021 climatology:

$$\alpha_{\text{std}} = \frac{\mu_i - \bar{\mu}}{\sigma} \quad (2)$$

where α_{std} denotes the standardized α , $\bar{\mu}$ is the average, and σ is the standard deviation of the variable α .

2.3.3. Linear Trends

We computed the linear trends using the Mann–Kendall trend test (Kendall’s coefficient, Z) to determine the significance of the trends and the Sen’s slope test to compute the magnitude of the trends [50,51]. These non-parametric methods assume datasets to have independent and random distribution. An advantage of using non-parametric estimators is that they can handle outliers and these methods are widely used in many areas [35,52]. All statistically significant trends were calculated using Student’s t -test at a 95% confidence level. For more details on the original M-K and Sen’s slope tests, refer to Mann [50] and Sen [51].

2.3.4. Correlation Analyses

We computed the correlation between country-wide maize production and climate anomalies from 1980 to 2021 based on Equation (3):

$$r = \frac{\sum_{i=1}^n (x_i - \bar{x})(y_i - \bar{y})}{\sqrt{\sum_{i=1}^n (x_i - \bar{x})^2 (y_i - \bar{y})^2}} \quad (3)$$

where r denotes the correlation coefficient, x_i denotes the climate variable, i denotes the time, and n denotes the sample size.

3. Results and Discussion

3.1. Annual Climatology and Trend Analysis

3.1.1. Climatology

Figure 2 displays the spatial distributions of the average annual values of E, Ep, PRE, SM, TMAX, and TMIN during the period 1980–2021. E and Ep ranged from 0.8 to 5.6 mm and from 1.6 to 5.6 mm, respectively. The annual mean daily PRE was 4.5 mm and ranged from 1 to 8 mm (Figure 2c). The PRE showed a higher rainfall distribution. The annual mean daily surface SM was $0.25 \text{ m}^3 \text{ m}^{-3}$ and varied between 0.06 and $0.45 \text{ m}^3 \text{ m}^{-3}$ (Figure 2d). The annual mean daily TMAX showed a mean of 28.8 and ranged from 20 to 37.5 °C (Figure 2e). The TMIN showed an annual daily mean of 17.5 °C and ranged from 10 to 25 °C (Figure 2f). Generally, a gradient was observed with high values in humid regions (i.e., 2 °N– 8 °N and 18 °W– 18 °E) followed by semi-arid regions (i.e., 8 °N– 14 °N) and low values in arid regions (14 – 20 °N) for E, Ep, PRE, and SM. On other hand, however, the temperature values TMAX and TMIN showed a latitudinal gradient: arid regions > semi-arid regions > humid regions (Figure 2e,d, respectively).

Figure 3 shows box plots of the annual cycles of E, Ep, PRE, SM, TMAX, and TMIN over the period 1980–2021. E displays a multi-year mean of 2.0 (range: 1 – 3.0 mm/day) (Figure 3a). Ep shows a mean value of 3.25 (range: 1 – 3.0 mm day^{−1}) (Figure 3b). PRE records a multi-year mean of 1.0 (0 – 2.0 mm day^{−1}) (Figure 3c). SM displays a multi-year mean of 0.175 (range: 0.125 – 0.225 m³m^{−3} day^{−1}). TMAX and TMIN show mean daily values of 32 (range: 28 – 36 °C) and 24 (range: 22 – 26 °C day^{−1}), respectively. The temporal pattern shows that E and Ep follow similar patterns, displaying high values in March and low values in July. PRE shows high values in November and low values in January. SM shows high values in November and low values in May. TMAX peaks from July to January, while TMIN peaks from August to January.

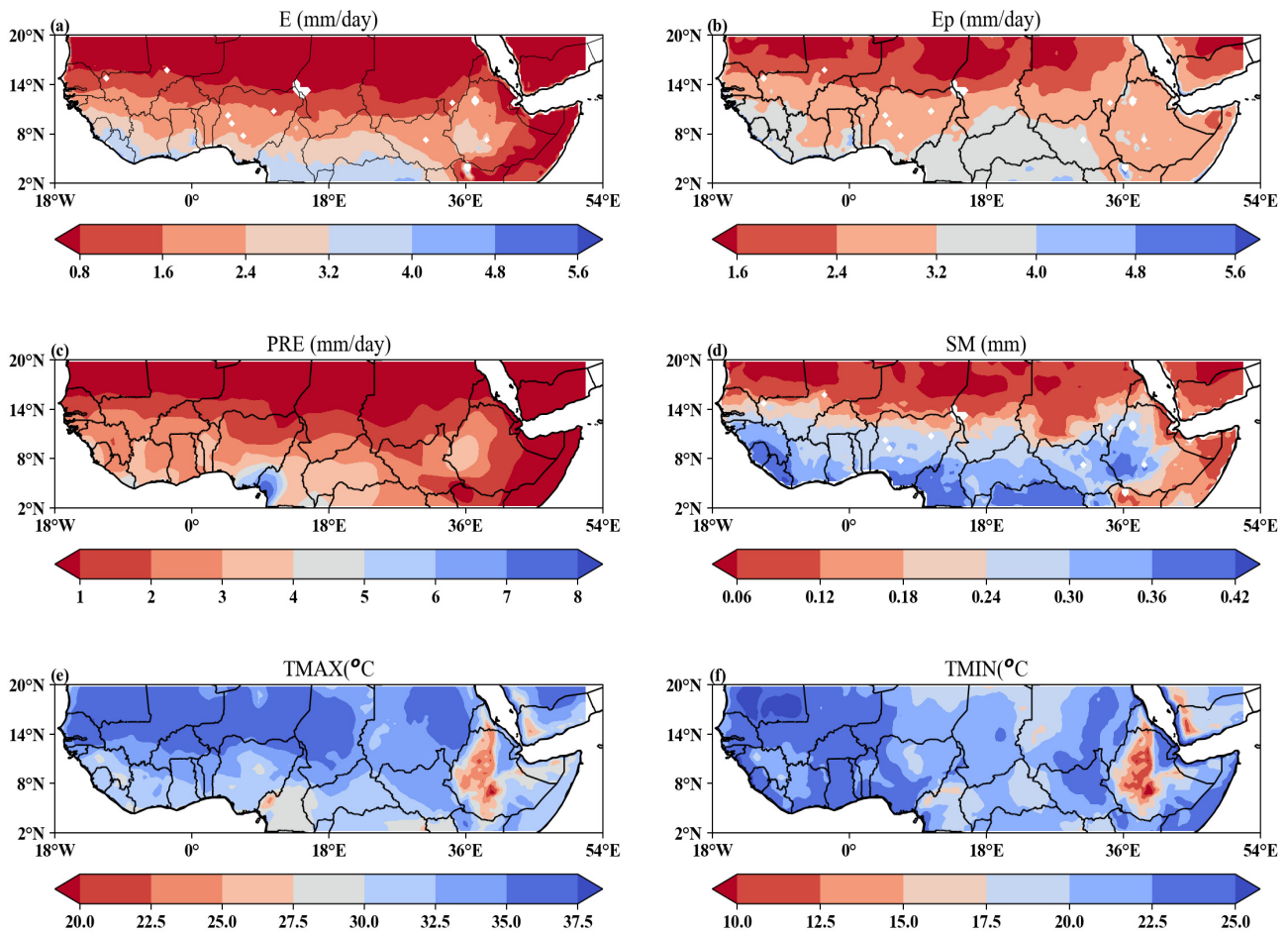


Figure 2. Spatial distribution of annual daily average (a) actual evapotranspiration (E), (b) potential evapotranspiration (Ep), (c) precipitation (PRE), (d) surface soil moisture (SM), (e) maximum temperature (TMAX), and (f) minimum temperature (TMIN) across Equatorial Africa (EQA) from 1980 to 2021.

3.1.2. Distribution of Annual Linear Climate Trends

Figure 4 shows the spatial patterns of the annual linear trends of E, Ep, PRE, SM, TMAX, and TMIN over the period 1980–2021. Overall, we observed a spatial heterogeneity of positive and negative trends across the study area. In arid regions, Ep (Figure 4b) displayed pronounced negative trends and E (Figure 4a) showed mixed trends. In semi-arid regions, the pattern of significant spatial trends for E and Ep were opposite (Figure 4a,c). For example, areas in the western Sahel (8°–14° N, 18° W–15° E) and central Sahel (8°–14° N, 15°–35° E) displayed positive and negative trends for E and Ep, respectively.

In humid regions, E and Ep showed similar spatial patterns with mixed trends along the Guinean coast (2°–8° N, 18° W–8° E) and the Horn of Africa (HOA) region (2°–8° N, 36°–52° E). We also observed opposite trends in E and Ep over the northern Congo Basin region (2°–8° N, 8°–35° E). The spatial patterns of PRE and SM importantly showed spatial heterogeneity, which could be due to a possible interaction between these two variables. For example, the semi-arid regions showed that PRE (Figure 4c) displayed no changing trends, while the SM (Figure 4d) displayed mixed trends (positive trends in the western and eastern Sahel, and negative trends in the central Sahel). Within the humid regions, negative trends were observed in small areas encompassing the Guinean coast and in the northern Congo Basin area (Figure 4c,d). The spatial patterns of linear trends in TMAX (Figure 4e) and TMIN (Figure 4f) showed generally similar results in the western EQCs (18° W–10° E). Meanwhile, opposite trends were evidenced in the region located between 10° and 52° E.

Figure 5 displays the annual temporal trends of E, Ep, PRE, SM, TMAX, and TMIN over the period 1980–2021. Generally, except for PRE, which exhibited a downward trend, the remaining variables displayed upward trends, albeit with differences in the magnitude of the trend values. E and Ep displayed upward trends of $0.03 \text{ mm (day}^{-1}10\text{a}^{-1})$ and $0.02 \text{ mm (day}^{-1}10\text{a}^{-1})$, respectively (Figure 5a,b). TMAX and TMIN showed a statistically significant increasing trend at $0.01 \text{ mm (day}^{-1}10\text{a}^{-1})$ (Figure 5c,d). In contrast, PRE exhibited a downward trend of $0.03 \text{ mm (day}^{-1}10\text{a}^{-1})$ (Figure 5c), while SM showed no change in trend (Figure 5d). Except for PRE and SM, all of the variables were statistically significant ($p < 0.05$).

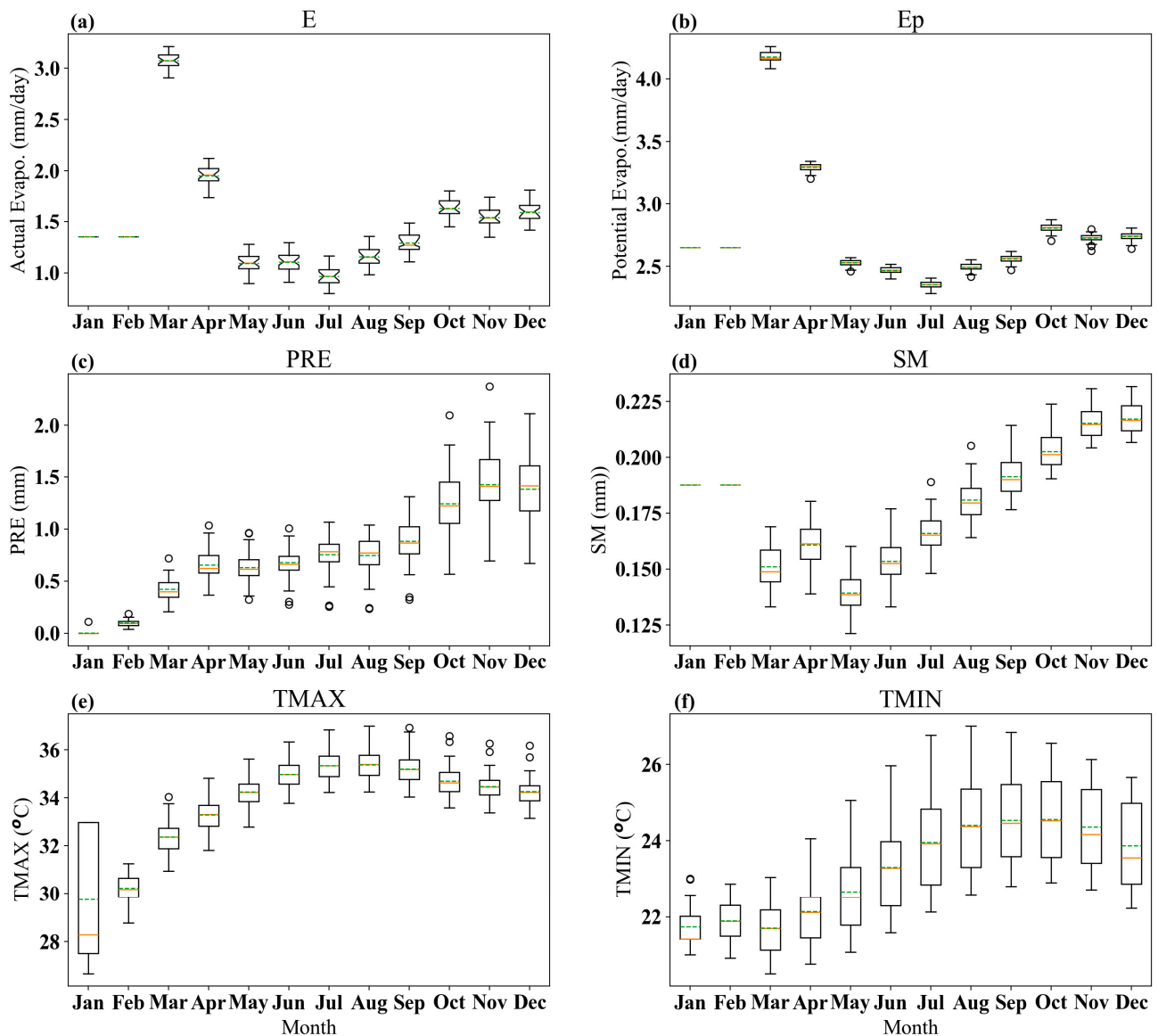


Figure 3. Box plots of the monthly climatology of (a) actual evapotranspiration (E), (b) potential evapotranspiration (Ep), (c) precipitation (PRE), (d) surface soil moisture (SM), (e) maximum temperature (TMAX), and (f) minimum temperature (TMIN) across Equatorial Africa (EQA) from 1980 to 2021. Error bars represent one standard deviation of uncertainty, while the circles represent the outliers. The green dashed lines and orange lines indicate the median values and mean values, respectively.

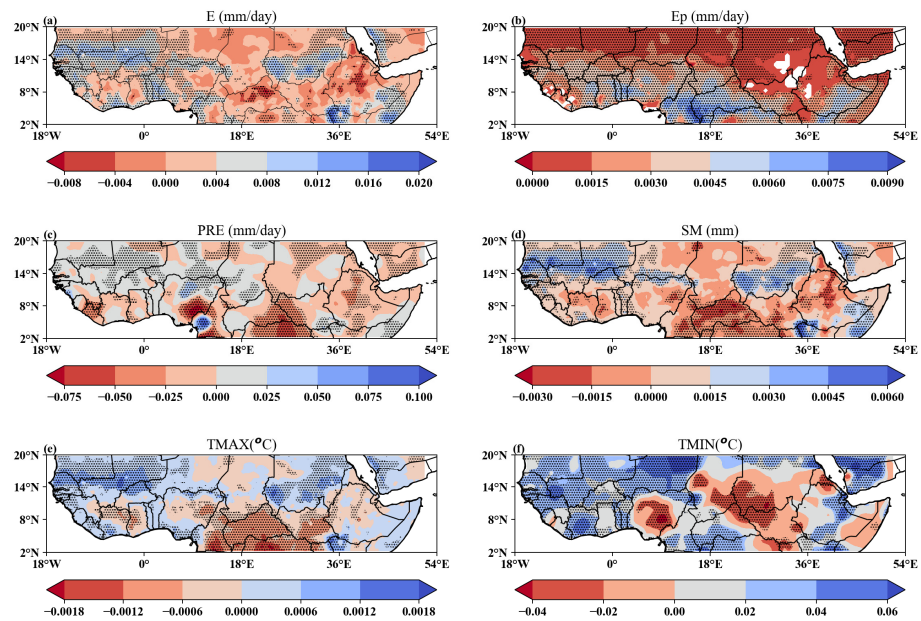


Figure 4. Spatial distribution of the linear trends of (a) actual evapotranspiration (E), (b) potential evapotranspiration (Ep), (c) precipitation (PRE), (d) surface soil moisture (SM), (e) maximum temperature (TMAX), and (f) minimum temperature (TMIN) across Equatorial Africa (EQA) from 1980 to 2021. The dots indicate areas with significant trends at a confidence level of 95%.

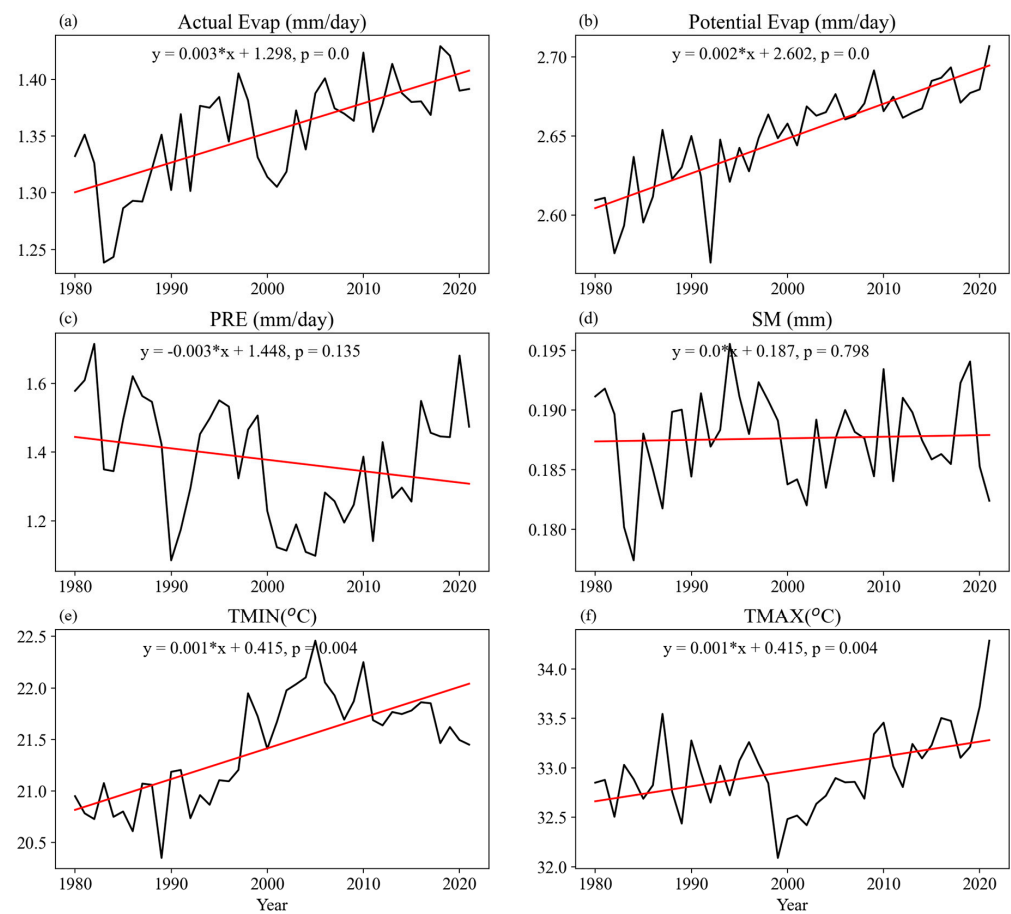


Figure 5. The same as Figure 4, but for the temporal linear trends.

3.1.3. Spatial Pattern of Wet–Dry Trends and Warm–Cool Trends

Figure 6 displays the spatial patterns of the wet–dry trends of E, Ep, PRE, and SM and the warm–cool trends of TMAX and TMIN from 1980 to 2021 based on the M-K test and the Sen's slope test. The annual wet–dry trends in the E and Ep values varied from -0.45 to $+0.6$ mm and from -0.30 to $+0.6$ mm (Figure 6a,b). Also, the PRE and SM annual trends ranged from -0.6 to $+0.45$ mm and from -0.6 to $+0.6$ m^3m^{-3} (Figure 6c,d), respectively. The annual warming and cooling trends in TMAX and TMIN varied between -0.60 and $+0.8$ °C. Generally, E and Ep showed similar patterns of wet-and-dry trends, except that opposite trends occurred in regions between 10°E and 52°E and in the Ethiopian Highlands (Figure 6a,b). PRE and SM exhibited similar patterns of wet-and-dry trends, except for the opposite trends observed in Sudan and the Arabian Peninsula (Figure 6c,d). The spatial distribution of TMAX (Figure 6e) and TMIN (Figure 6f) showed similar patterns of warm-and-cool trends, except for the divergent trends observed in Ghana, Mali, Nigeria, Chad, Sudan, South Sudan, and Somalia.

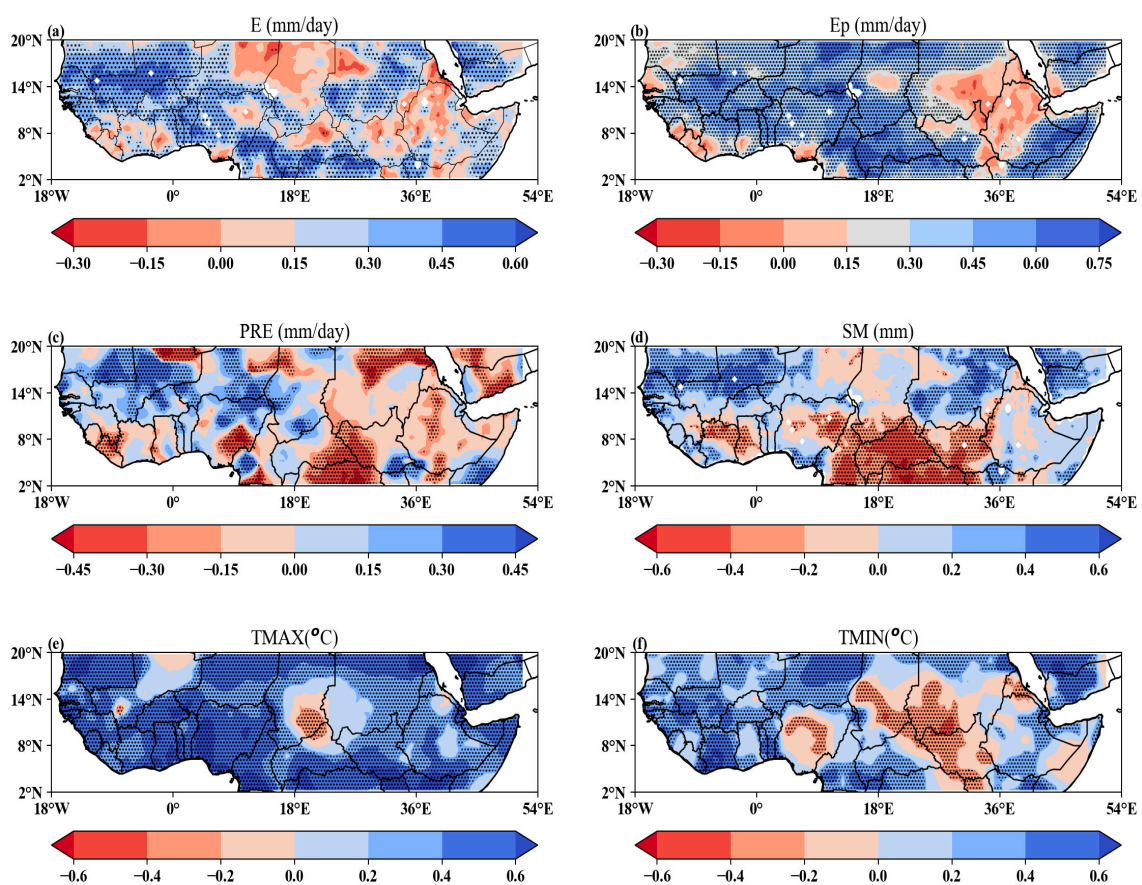


Figure 6. Spatial patterns of the M-K trends of (a) actual evapotranspiration (E), (b) potential evapotranspiration (Ep), (c) precipitation (PRE), (d) surface soil moisture (SM), (e) maximum temperature (TMAX), and (f) minimum temperature (TMIN) across Equatorial Africa (EQA) from 1980 to 2021. The unit is mm d^{-1} . Analyzed based on the MK and Sen's slope tests. The red and blue colors denote decreasing and increasing trends, respectively. The dots denote the regions where the trends are statistically significant at a confidence level of 95%.

3.2. Overall and Country-Level Time-Series Analyses

3.2.1. Country-Level Maize Production and Yield Estimates

Figure 7 presents a time-series analysis of the maize production, yield, and harvested land area in selected countries located in the study area. High year-to-year variability is displayed in the maize production (Figure 7, line graph) and harvested area (Figure 7, bar graph).

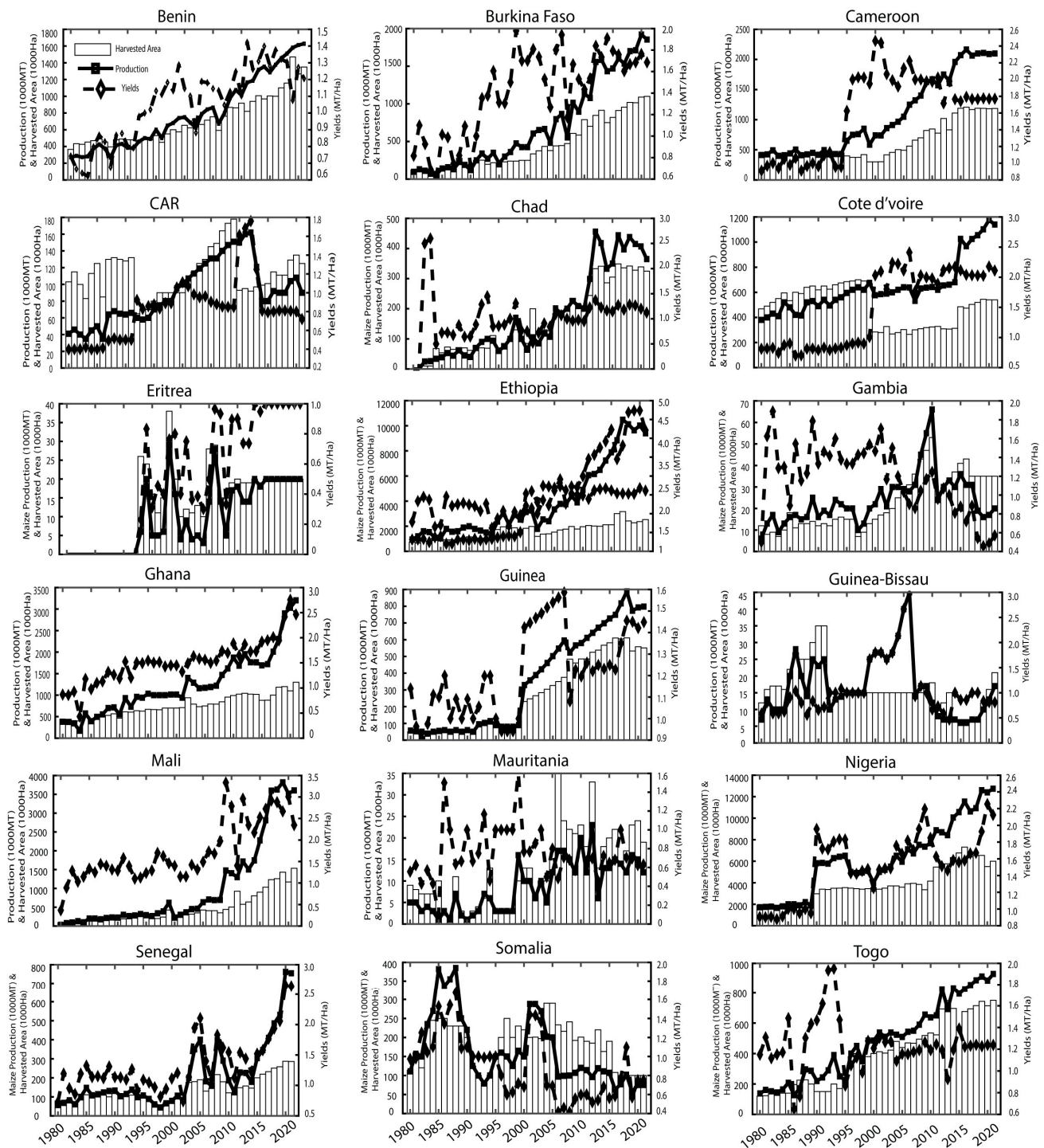


Figure 7. Changes in maize production (MT), harvested land area (HA), and yield (MT/ha). The dotted and dashed lines in the plots denote the linear trends of the maize production and yields, respectively; the bar plots indicate the harvested area during 1980 to 2021.

The maize yield behavior, depicted in Figure 7, was highly variable between the countries and years, with most countries displaying relatively stable yields (Benin, Burkina Faso, Cameroon, Cote d’Ivoire, Chad, Ghana, Guinea, Mali, Ethiopia, Nigeria, Senegal, Somalia, and Togo) throughout time. Few countries displayed strong fluctuations (e.g., Guinea-Bissau, the CAR, Mauritania, Eritrea, Somalia, and Gambia). The consistently higher maize production across the EQCs corroborates other studies that support maize as one of the vital food crops in this region [20,25] and other global land areas [53–55].

3.2.2. Descriptive Statistics of Annual Maize and Climate

To reveal the temporal differences in maize production and hydro-climate trends, the mean (standard deviation) values were computed for the selected countries from 1980 to 2021 (Table 2). Overall, Nigeria presented the largest average maize production of 6221.7 ± 3325.8 MT. The annual daily climate variables for Nigeria were SM ($0.27 \pm 0.09 \text{ m}^3\text{m}^{-3}$), PRE (2.92 ± 2.9 mm), TMIN (22.8 °C), TMAX (33.19 ± 2.9 °C), E (2.06 ± 0.9 mm), and Ep (3.05 mm). The overall statistics across the EQCs ranged between 0.45×10^4 and 3.8×10^4 (MT); the harvested area was between 0.50×10^4 and 4×10^4 ha; and the yield was between 12 and 28 (MT/ha) (Figure A1).

The country with the least maize production was Mauritania, with an average value of 8.715 ± 5.923 MT (Table 2). The climate variables for Mauritania showed the following values: SM ($0.53 \pm 0.04 \text{ m}^3\text{m}^{-3}$), PRE (0.428 ± 0.895 mm), TMIN (24.915 °C), TMAX (36.023 ± 4.643 °C), E (0.224 ± 0.407 mm), and Ep (1.567 ± 0.440 mm) (Table 2). The remaining production and hydro-climate data are shown in Table 2 for the rest of the countries.

3.2.3. Country-Wide Trend Analysis of Climate Variables

Table 3 presents the trends in the hydro-climate variables, expressed according to the M-K test (Z) and Theil–Sen slope (β) values on an annual scale and a growing-season scale. Here, we present Z values that were statistically significant at $\alpha = 0.05$. Most national annual climate parameters remained generally stable (trends without statistical significance). Our results focus on countries that experienced statistically significant positive/negative trends.

Precipitation exhibited significant increasing trends in a few countries, such as Burkina Faso ($Z = 2.449 \text{ yr}^{-1}$), Mali ($Z = 1.972 \text{ yr}^{-1}$), and Mauritania ($Z = 2.275 \text{ yr}^{-1}$) ($p < 0.05$), on the annual scale. Soil moisture showed increasing trends in Burkina Faso ($Z = 3.641 \text{ yr}^{-1}$), Gambia ($Z = 2.275 \text{ yr}^{-1}$), Guinea-Bissau ($Z = 4.010 \text{ yr}^{-1}$), Mali ($Z = 3.663 \text{ yr}^{-1}$), and Senegal ($Z = 4.053 \text{ yr}^{-1}$), while decreasing trends were observed in Cameroon ($Z = -4.313 \text{ yr}^{-1}$), the CAR ($Z = 5.310 \text{ yr}^{-1}$), Ghana ($Z = -1.972 \text{ yr}^{-1}$), and Mauritania ($Z = -5.310 \text{ yr}^{-1}$) on the annual scale. Both E and Ep showed similar increasing trends in Benin, Burkina Faso, Cote d'Ivoire, Guinea-Bissau, Mali, Mauritania, Nigeria, Senegal, Somalia, and Togo. Also, Ep increased in Cameroon, the CAR, Chad, Ghana, and Guinea on the annual scale. TMAX and TMIN displayed statistically increasing trends in Benin, Burkina Faso, Guinea-Bissau, Cote d'Ivoire, Senegal, Mali, Mauritania, and Togo ($p < 0.05$). However, TMAX also showed statistical significance in Ghana and Guinea. TMIN showed significant values in Cameroon, Chad, Eritrea, Ethiopia, Nigeria, and Somalia.

During the growing seasons, PRE increased significantly in Burkina Faso, Cote d'Ivoire, Ghana, Guinea, Guinea-Bissau, Mali, and Mauritania ($p < 0.05$). SM increased significantly in Burkina Faso, Eritrea, Gambia, Guinea-Bissau, Mali, Mauritania, and Senegal, while displaying negative trends in Cameroon, the CAR, and Ghana. E and Ep showed increasing trends in Benin, Burkina Faso, Cameroon, the CAR, Cote d'Ivoire, Ethiopia, Ghana, Guinea, Guinea-Bissau, Mali, Mauritania, Nigeria, Senegal, Somalia, and Togo. However, some countries showed increasing trends for E (Gambia) and Ep (Chad). TMAX and TMIN showed similar increasing trends in Benin, Burkina Faso, Cameroon, Cote d'Ivoire, Ghana, Guinea, Guinea-Bissau, and Mauritania. However, increasing trends were found for TMAX in Chad and Mali, and for TMIN in Gambia, Nigeria, Senegal, Somalia, and Togo. All trends were statistically significant ($p < 0.05$).

Table 2. Descriptive statistics of annual maize production and climate variables during 1980–2021.

Country	Maize (tons)	TMIN (°C day ⁻¹)	TMAX (°C day ⁻¹)	SM (m ³ m ⁻³ day ⁻¹)	E (mm day ⁻¹)	Ep (mm day ⁻¹)	PRE (mm day ⁻¹)
Benin	713.333 ± 594.865	22.854 ± 2.06	33.19 ± 2.987	0.276 ± 0.079	2.064 ± 0.921	3.047 ± 0.415	2.915 ± 2.905
Burkina Faso	1055.524 ± 645.654	23.271 ± 3.333	35.545 ± 3.137	0.200 ± 0.088	1.335 ± 1.012	2.627 ± 0.504	1.945 ± 2.564
Cameroon	1055.524 ± 645.654	20.116 ± 2.693	29.781 ± 3.04	0.344 ± 0.082	2.826 ± 0.947	3.369 ± 0.415	3.942 ± 3.922
Chad	172.571 ± 146.106	21.059 ± 4.672	35.121 ± 4.395	0.132 ± 0.101	0.694 ± 1.001	2.182 ± 0.818	0.96 ± 1.851
Cote D'Ivoire	644.738 ± 210.331	22.68 ± 1.676	32.279 ± 2.39	0.297 ± 0.068	2.519 ± 0.898	3.224 ± 0.482	3.012 ± 2.713
Eritrea	9.857 ± 9.127	20.464 ± 4.623	31.627 ± 4.683	0.137 ± 0.075	1.111 ± 1.488	2.942 ± 0.891	0.783 ± 1.406
Ethiopia	3930.738 ± 2956.233	19.571 ± 4.978	29.681 ± 4.039	0.171 ± 0.082	1.072 ± 0.936	2.893 ± 0.524	0.991 ± 1.568
Gambia	23.833 ± 11.603	23.074 ± 3.041	35.305 ± 2.742	0.239 ± 0.084	1.470 ± 1.051	3.022 ± 0.492	1.845 ± 2.887
Ghana	1243.952 ± 723.268	23.535 ± 1.689	32.143 ± 2.725	0.292 ± 0.074	2.578 ± 1.010	3.258 ± 0.578	2.637 ± 2.429
Guinea	352.524 ± 297.549	22.213 ± 3.119	31.817 ± 2.824	0.328 ± 0.095	2.361 ± 1.032	3.349 ± 0.515	2.519 ± 3.612
Guinea-Bissau	16.786 ± 9.307	23.671 ± 2.99	34.018 ± 2.633	0.293 ± 0.094	2.021 ± 1.099	3.291 ± 0.563	2.447 ± 3.637
Mali	992.333 ± 1166.772	23.406 ± 4.316	35.468 ± 4.069	0.148 ± 0.112	0.934 ± 1.037	2.238 ± 0.749	1.36 ± 2.262
Mauritania	8.714 ± 5.923	24.915 ± 4.914	36.023 ± 4.643	0.053 ± 0.04	0.224 ± 0.407	1.567 ± 0.440	0.428 ± 0.895
Nigeria	6221.667 ± 3325.835	21.472 ± 3.338	32.027 ± 3.71	0.275 ± 0.112	1.983 ± 1.103	2.887 ± 0.543	2.787 ± 3.559
CAR	90.190 ± 36.428	19.985 ± 2.534	31.65 ± 2.865	0.308 ± 0.076	2.640 ± 0.980	3.403 ± 0.282	3.153 ± 3.015
Senegal	207.690 ± 176.352	23.357 ± 3.29	35.801 ± 3.2	0.179 ± 0.095	1.250 ± 1.123	2.679 ± 0.739	1.416 ± 2.483
Somalia	164.786 ± 90.790	21.982 ± 2.842	30.724 ± 2.518	0.119 ± 0.047	0.666 ± 0.926	2.799 ± 0.631	0.357 ± 0.659
Togo	483.952 ± 256.502	22.64 ± 1.717	32.539 ± 2.735	0.287 ± 0.077	2.335 ± 0.853	3.202 ± 0.422	2.937 ± 2.739

Table 3. Country-level summary statistics according to the M-K test (Z) and Sen’s slope estimator (β), annually and in the growing seasons, for the maize and climate variables over the period 1980–2021. * = significance level at 0.01 < α ≤ 0.05. The beta coefficient (β) indicates the changes per year or changes per growing season.

Climate Variables		Annual						Growing Seasons					
		SM	Tmax	Tmin	E	EP	P	P	Tmax	Tmin	E	EP	SM
Benin	Z	1.821	4.595 *	4.66 *	5.072 *	5.397 *	0.910	1.641	4.710	2.640	5.029	4.811	1.257
	β	0.0002	0.025	0.022	0.0066	0.0042	0.0030	0.0149	0.0332	0.0145	0.0063	0.0046	0.0002
Burkina	Z	3.641 *	3.294 *	4.530 *	4.963 *	5.071 *	2.449 *	3.175 *	2.640 *	2.212 *	4.660 *	4.400 *	3.338 *
	β	0.0006	0.020	0.025	0.0072	0.0025	0.0080	0.0246	0.0220	0.0165	0.0074	0.0029	0.0006
Cameroon	Z	-4.313 *	1.408	5.158 *	2.406	5.917 *	-1.972	-1.178	2.462 *	3.176 *	4.443 *	5.375 *	-4.660 *
	β	-0.0006	0.012	0.031	0.0021	0.0050	-0.0155	-0.0196	0.0504	0.0271	0.0042	0.0059	-0.0007
CAR	Z	-5.310 *	1.864	1.712	-0.542	6.307 *	-0.672	0.393	1.927	1.178	2.796 *	5.527 *	-5.180 *
	β	-0.0008	0.016	0.011	-0.0006	0.0052	-0.0053	0.0069	0.0235	0.0164	0.0029	0.0061	-0.0009

Table 3. Cont.

Climate Variables		SM	Tmax	Annual				Growing Seasons					
				Tmin	E	EP	P	P	Tmax	Tmin	E	EP	SM
Chad	Z	−0.368	−0.216	4.140 *	0.564	6.567 *	1.040	1.606	2.569 *	−0.357	0.801	6.069 *	−0.607
	β	−0.0000	−0.002	0.023	0.0010	0.0018	0028	0.0099	0.0409	−0.0072	0.0014	0.0022	−0.0001
Cote D'Ivoire	Z	−1.127	5.483 *	3.208 *	2.232 *	5.029 *	0.152	3.033 *	4.781 *	2.212 *	2.406 *	3.728 *	−1.907
	β	−0.0001	0.032	0.033	0.0029	0.0035	0.0011	0.0249	0.0353	0.0185	0.0025	0.0035	−0.0003
Eritrea	Z	0.065	−1.235	5.115 *	0.217	2.688 *	−1.366	−0.107	0.535	0.178	0.477	0.867	0.216
	β	0.0000	−0.009	0.040	0.0003	0.0008	−0.0065	−0.0006	0.0062	0.0029	0.0010	0.0004	4.3195 *
Ethiopia	Z	−0.433	0.455	4.985 *	0.715	5.202 *	−1.712	−0.856	1.855	0.749	1.972 *	5.310 *	0.347
	β	−0.0001	0.003	0.071	0.0013	0.0027	−0.0072	−0.0063	0.0207	0.0085	0.0033	0.0026	0.0001
Gambia	Z	2.275 *	1.539	5.115	2.753	1.300	−0.347	0.071	1.784	3.283 *	2.037 *	−0.195	1.951 *
	β	0.0003	0.011	0.040	0.0032	0.0007	−0.0031	0.0020	0.0311	0.0726	0.0036	−0.0001	0.0003
Ghana	Z	−1.972 *	1.972 *	3.815	1.560	4.790 *	−1.019	1.820	3.604 *	3.211 *	2.059 *	3.641 *	−2.341 *
	β	−0.0003	0.016	0.055	0.0018	0.0036	−0.0033	0.0141	0.0541	0.0312	0.0025	0.0033	−0.0003
Guinea	Z	1.474	3.706 *	5.765	3.663	4.269 *	1.084	2.997 *	3.033 *	2.212 *	3.360 *	3.576 *	0.975
	β	0.0001	0.030	0.105	0.0047	0.0029	0.0075	0.0594	0.0430	0.0522	0.0042	0.0033	0.0001
Guinea-Bissau	Z	4.010 *	4.270 *	3.901 *	5.353 *	3.858 *	0.759	−0.678	2.640 *	4.460 *	3.771 *	3.316 *	2.948 *
	β	0.0004	0.027	0.028	0.0069	0.0026	0.0057	−0.0084	0.0306	0.1179	0.0061	0.0027	0.0004
Mali	Z	3.663 *	3.425 *	5.917 *	5.180 *	6.199 *	1.972 *	3.033 *	3.925 *	1.392	5.310 *	5.765 *	3.381 *
	β	0.0004	0.027	0.088	0.0054	0.0019	0.0063	0.0226	0.0480	0.0134	0.0066	0.0023	0.0004
Mauritania	Z	−5.310 *	2.774 *	5.397 *	3.836 *	3.165 *	2.275 *	1.320	2.855 *	4.246 *	3.576 *	2.622 *	3.576 *
	β	−0.0008	0.025	0.037	0.0035	0.0006	0.0051	0.0088	0.0429	0.0933	0.0047	0.0006	0.0004
Nigeria	Z	−0.866	−0.303	3.468 *	4.053 *	5.440 *	−1.170	−1.035	0.785	3.818 *	4.226 *	4.855 *	−1.777
	β	0.0001	−0.002	0.022	0.0028	0.0033	−0.0068	−0.0088	0.0181	0.0368	0.0035	0.0038	−0.0002
Senegal	Z	4.053 *	3.858 *	4.833 *	5.115 *	3.034 *	1.495	1.570	3.604	3.390 *	4.638 *	2.233 *	3.576 *
	β	0.0006	0.032	0.045	0.0067	0.0012	0.0056	0.0139	0.0468	0.0441	0.0072	0.0009	0.0006
Somalia	Z	1.452	−0.867	2.818 *	2.796 *	5.332 *	0.087	−1.142	1.142	2.748 *	2.969 *	5.787 *	1.626
	β	0.0001	−0.008	0.023	0.0044	0.0026	0.0003	−0.0041	0.0177	0.0334	0.0057	0.0031	0.0002
Togo	Z	0.122	4.118 *	4.508 *	4.552 *	5.440 *	0.694	2.177 *	4.888	3.211 *	4.660 *	4.725 *	0.954
	β	0.0002	0.022	0.024	0.0065	0.0046	0.0031	0.0223	0.0409	0.0189	0.0061	0.0048	0.0002

3.2.4. Statistical Relationship between Maize Production and the Climate

Figure 8 shows the heat-map plots of the correlation coefficient (r) computed between the country-level maize production and climate anomalies. The results showed that the highest correlation was recorded for maize and TMAX (0.77) in Cote d’Ivoire, and the lowest was recorded for maize and PRE (−0.01) in Guinea-Bissau. SM and maize showed mixed correlation results, with a positive correlation in Burkina Faso (0.52), Gambia (0.67), Mali (0.45), Mauritania (0.59), and Senegal (0.43) and a negative correlation in Cameroon (−0.60) and the CAR (−0.64). The remaining correlation coefficient (r) values were insignificant at the 95% confidence level. On the other hand, PRE and maize displayed a moderately positive correlation coefficient (r) for Burkina Faso (0.47), Chad (0.43), Mali (0.58), and Senegal (0.48).

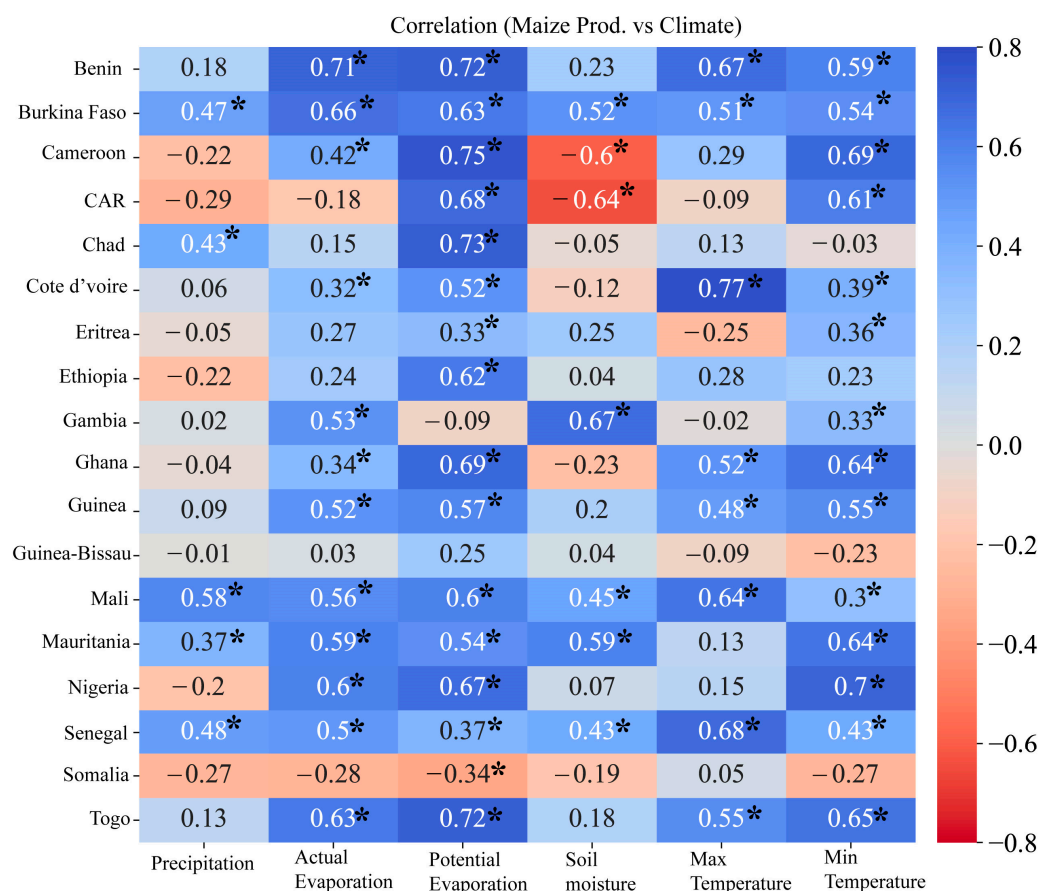


Figure 8. Heat map of Pearson correlation coefficient (r) values between the annual maize production and hydro-climate variables. * denote statistical significance at $p < 0.05$.

Regarding E and Ep, our results showed a significant positive correlation with maize production in Benin, Burkina Faso, Cameroon, Cote d’Ivoire, Ghana, Guinea, Mali, Mauritania, Nigeria, Senegal, and Togo. However, only a few countries showed a significant positive correlation with E (Gambia) or Ep (Ethiopia, Eritrea, Chad), and a negative one was observed for Somalia (Ep). Similarly, a significant positive correlation was found for the temperature variables (TMIN and TMAX) in Benin, Burkina Faso, Cote d’Ivoire, Ghana, Guinea, Mali, and Togo. TMIN also showed a positive trend for Cameroon, the CAR, Eritrea, Gambia, Mauritania, and Nigeria. All trends were statistically significant at the $\alpha = 0.05$ level.

4. Discussion

Climate change and natural variability threatens agricultural crop production, especially in water- and energy-limited regions, where food crops are rainfed and harvested through subsistence farming by small-holder farmers.

We investigated the climatology and linear trends of six hydro-climate variables and their impacts on maize production in selected countries located in the Equatorial Africa region. The spatial pattern analysis captured and revealed the observed climatology and observed trends of hydro-climate variables across the study area to be consistent with those reported in a past study [28]. Some locations were captured with more pronounced rainfall patterns and less pronounced temperature patterns, or vice versa. The EQCs showed annual cycles of precipitation (with amounts ranging from 0 to 2.0 mm day⁻¹) and temperatures (i.e., maximum air surface temperatures between 20 and 38 °C day⁻¹ and minimum air surface temperatures in the range of 10 and 25 °C day⁻¹) that are consistent with the ideal rainfall and temperatures for maize crop production [56]. According to the FAO [9], the sowing seasons are in May–August and September to December; however, the intra-annual variability captured in this study did not show that pattern. This could be due to the area-averaged values we applied or the selected region not being similar to that used by the FAO. The annual monthly distributions of the hydro-climate variables suggest that the maize crop could have at least two cropping calendars [13,24]. Maize is one of the most widely grown crops in EQA, which encompasses arid regions that transition through to rainforest regions [57]. Spatially, the precipitation displayed significant positive changes mostly in the Sahel region, meaning that the Sahel experienced increases in precipitation. This confirms the earlier findings for this region. The southern part of the Sahel (Guinea Coast) experienced negative trends, thus culminating in an average negative trend of 0.03 mm/10a⁻¹, consistent with previous regional studies [30,58]. Linear trends in the soil moisture show an augmentation in the region's precipitation over certain regions and a reduction in it in arid and humid regions, which is in line with past studies [59–61]. The spatial pattern of evapotranspiration showed similar trends for actual and potential evapotranspiration. However, both types of evapotranspiration increased at rates of 0.03 mm/10a⁻¹ and 0.02 mm/10a⁻¹, respectively. In the context of a warming climate, increasing evapotranspiration may lead to an increase in surface water losses and increased water availability, as supported by previous studies [37,52,62]. The spatial patterns of the minimum and maximum temperatures showed heterogeneity in their trends, but the overall values showed an identical trend rate of 0.01 °C 10a⁻¹. Our results are supported by previous regional studies [30,63,64] and studies on global climate patterns [1,5]. TMAX and TMIN were reported with rates of 1.9 °C and 1.2 °C in East Africa by Gebrechorkos, Hülsmann and Bernhofer [30], and rates of 0.2 °C 10a⁻¹ for the mean minimum temperature and 0.10 °C 10a⁻¹ for the mean maximum temperature were reported in the IPCC AR5 report [5]. Overall, the values of trends and their significance depend on the region and time period under consideration [31]. Although the results of the temporal pattern analysis (Figure 7) of annual maize production differed among the EQCs (Table 2), the mean (standard deviation) climatic variables suggest good ideal conditions for maize production, which largely explains the popularity of maize production in this region, as maize is a staple food in the region [20,25] and throughout the world [53–55]. The quantity of maize produced by each country maybe explains the largely high inter-annual variations in the harvested area. Nigeria and Mauritania produced the highest and lowest amount of maize over the four decades (i.e., 1980–2021). Maize cultivation in many of these countries is rainfed and the yields of maize are maybe impacted by the harvested area. The harvested area mostly influences decisions on the space (i.e., where) and time (i.e., when) to grow crops [16]. This in turn is partly due to a combination of different hydro-climate variables [55] or other limiting factors (e.g., the number of crops grown, the maize survival rate, the sowing date [16,17], general farming inputs (e.g., investments [65,66]) or profitability [6], technology [11,67], improved seed varieties [23], or fertilizer applications [68]). At the national level, the spatial pattern analysis showed significant ($p < 0.05$) wetting and warming

over Burkina Faso, Mali, Mauritania, Senegal, Gambia, Guinea-Bissau, and Togo (Table 3). Also, the country-level analysis showed that the drying and warming over Benin, Ghana, Cameroon, and the CAR was significant at $\alpha = 0.05$ (Table 3). Wet and warm conditions are essential in promoting agricultural development due to crops' water requirements [57,69]. Our correlation analysis showed that the climate drivers' influence on maize production differed from country to country. Focusing on countries with significant values, Burkina Faso, Chad, Mali, and Senegal showed their maize production and precipitation to be positively correlated. Soil moisture was negatively correlated in Cameroon and the CAR, and positively correlated in Burkina Faso, Gambia, Mali, and Mauritania. Our analyses suggested that maize production is highly sensitive to different water conditions, which may influence the sowing dates [16,17]. The temperature's correlation with maize showed a strongly positive correlation in nearly all of the countries (significant at $p < 0.05$), which is not surprising. These findings are supported by studies reporting that temperatures (i.e., minimum and maximum) control plant metabolism [32,70], where maximum temperatures enhance plant photosynthesis and minimum temperatures improve plant respiration and nutrient consumption to subsequently increase crop production (or yields) [71]. However, countries that exhibit weakly negative and non-significant correlations between maize and precipitation and soil moisture may be prone to flash droughts. This is consistent with the regions that experienced high inter-annual variations in precipitation (Figures 4–6), with higher temperatures (Figure 4e,f) and water loss through ET (Figure 4a,b) further exacerbating the soil moisture conditions (Figure 4d) when there was a lack of precipitation (Figures 4c and 5c). Our findings confirmed that evapotranspiration, minimum and maximum temperatures, and soil moisture influence maize production across the EQCs. Overall, our correlation analysis showed that climate drivers impact maize production differently across the countries considered, thus suggesting the need for tailor-made responsive measures, consistent with the literature [22,72,73]. The correlation analysis indicated that maize production in many of the studied regions is related to the trends of these climate drivers [22]. Additional analyses showed that large-scale climatic phenomena such as the El Niño Southern Oscillation (ENSO) also influence maize production (Figures S1–S5).

Previous research on climate drivers' impacts on crop production has focused largely on mean temperatures and precipitation in different parts of SSA [7,22]. However, there is limited research examining other factors such as evapotranspiration, temperatures (i.e., minimum and maximum), and soil moisture in the Equatorial Africa region. This study has analyzed the influence of climate variability on maize production. Also, we have explored the effects of other factors such as evapotranspiration, temperatures (i.e., minimum and maximum), and soil moisture on maize production. Future studies should quantify the relationship between climate change and crop production and examine the causality of the trends in climatic factors and global warming affecting maize production.

In summary, climate drivers mostly influence farmers' decisions on where (i.e., space) and when (i.e., time) to grow crops in rainfed regions. This study, consistent with previous studies, demonstrated that climate change influences maize production [20,74]. However, we advise readers to treat these findings with caution as there are other unexplained limiting factors. Maize production is known to be influenced by factors such as the maize variety [23,25,68,75], technological investments [25,66,67], etc. Our study contributes to the ongoing discussion on the state of Africa's warming climate and its impact on different sectors of the economy. This study provides in-depth analyses of country-wide spatio-temporal changes in climate patterns in relation to maize production. These country-wide analyses are vital for effectively managing agricultural systems, and provide a scientific basis for adapting tailored policies and programs in rainfed agricultural regions.

5. Conclusions

The existing research on the effects of hydro-climate parameters on maize production over Equatorial African countries, especially considering country-wide analyses, is very limited. Hence, this study analyzed changes in hydro-climate variables (i.e., actual (E) and

potential (Ep) evapotranspiration, precipitation (PRE), soil moisture (SM), and minimum (TMIN) and maximum (TMAX) temperatures) over Equatorial African countries to quantify trends and assess the interdependence of these climatic variables with maize production over the 1980–2021 time period. The main conclusions are summarized as follows:

The area average of precipitation over Equatorial Africa decreased significantly over the studied period, whereas the soil moisture, temperatures (maximum and minimum), and evapotranspiration increased with varying significance.

Our spatial trend analysis showed heterogeneous changes in all variables. The country-wide analysis showed that the minimum temperature increased. While the maximum temperature decreased in some countries, it increased in most of the countries. The precipitation increased in most of the countries (except Cameroon, the CAR, Eritrea, Ethiopia, Gambia, Ghana, and Nigeria) on an annual scale, while during the growing seasons, these countries experienced reductions in precipitation, as well as Guinea-Bissau and Somalia.

The relationship of hydro-climate variables with the maize production in each country was revealed to be mostly strong, except for the countries where the precipitation declined. This suggests that many other parameters influence the maize production in EQCs. Further studies would be needed to uncover the most influential variables. These findings are helpful for water resource management and food security.

Supplementary Materials: The following supporting information can be downloaded at <https://www.mdpi.com/article/10.3390/atmos15050542/s1>: Figure S1. Trends in maize production anomalies in response to E and teleconnection (SST and El Niño, 3.4 index). Figure S2. Trends in maize production anomalies in response to Ep and teleconnection (SST and El Niño, 3.4 index). Figure S3. Trends in maize production anomalies in response to PRE and teleconnection (SST and El Niño, 3.4 index). Figure S4. Trends in maize production anomalies in response to SM and teleconnection (SST and El Niño, 3.4 index). Figure S5. Trends in maize production anomalies in response to SM and teleconnection (SST and El Niño, 3.4 index).

Author Contributions: Conceptualization, I.K.N., F.K.O. and J.L.; methodology, I.K.N. and F.K.O.; software, I.K.N. and F.K.O.; validation, I.K.N., F.K.O. and J.L.; formal analysis, I.K.N. and F.K.O.; investigation, I.K.N. and F.K.O.; data curation, I.K.N., F.K.O., N.A.P. and A.A.S.C.; writing—original draft preparation, I.K.N.; writing—review and editing, N.A.P., D.F.T.H., Z.J., F.M.N. and A.A.S.C.; visualization, N.A.P., D.F.T.H., Z.J., F.M.N. and A.A.S.C. All authors have read and agreed to the published version of the manuscript.

Funding: This research was funded by the Wuxi University Starting Project 2021r010.

Institutional Review Board Statement: Not applicable.

Informed Consent Statement: Not applicable.

Data Availability Statement: Data available in a publicly accessible repository that does not issue DOIs. Publicly available datasets were analyzed in this study. This data can be found here: [GLEAM evapotranspiration (www.GLEAM.eu 29 March 2024), NOAA climate indices (<ftp://ftp.cdc.noaa.gov/Datasets> 29 March 2024), NASA SRTM DEM (<https://lpdaac.usgs.gov/products/srtmgl1v003/> 29 March 2024), USDA (<https://www.indexmundi.com/agriculture/> 29 March 2024).

Acknowledgments: We are very grateful to the institutions for making their datasets available for use in accordance with their specific data-use and citation policies: We acknowledge the technical support provided by the medical imaging platform with the CMOS image sensor (Wuxi Univ Starting Project 2021r010) and the design of minimally invasive surgery robot project by the School of Atmospheric Science and Remote Sensing, Wuxi University.

Conflicts of Interest: The authors declare no conflicts of interest.

Appendix A

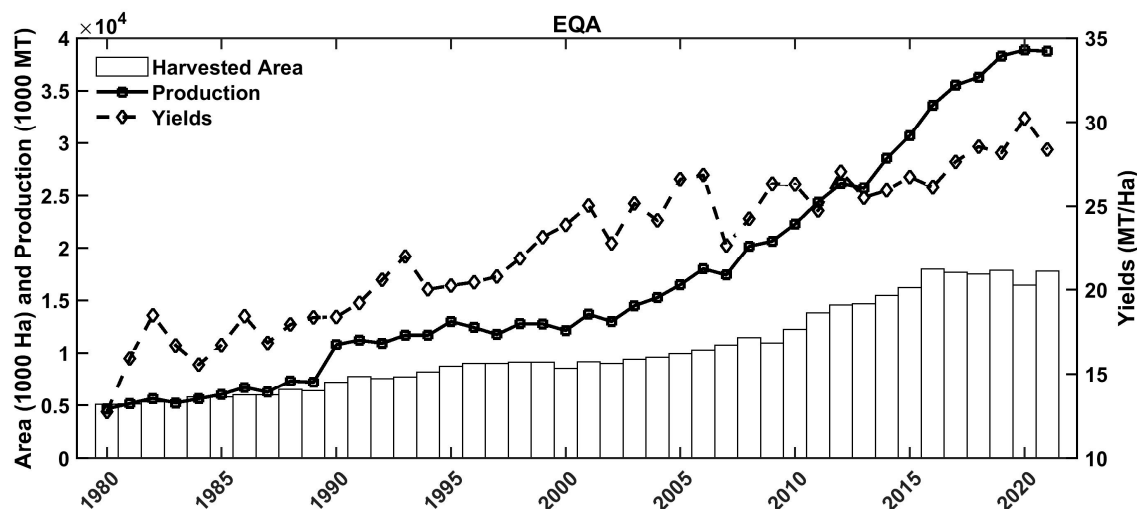


Figure A1. Changes in maize production (MT), harvested land area (ha), and yield (MT/ha) in Equatorial African countries (EQCs). The dotted and dashed lines in the plots denote the linear trends for maize production and yields, respectively; the bar plots indicate the harvested area during 1980 to 2021.

References

1. IPCC. *Climate Change 2021: The Physical Science Basis*; IPCC: Geneva, Switzerland; Cambridge University Press: Cambridge, UK, 2021.
2. Vogel, E.; Meyer, R. Chapter 3—Climate Change, Climate Extremes, and Global Food Production—Adaptation in the Agricultural Sector. In *Resilience*; Zommers, Z., Alverson, K., Eds.; Elsevier: Amsterdam, The Netherlands, 2018; pp. 31–49.
3. Karl, T.R.; Melillo, J.M.; Peterson, T.C. *Global Climate Change Impacts in the United States*; Cambridge University Press: Cambridge, UK, 2009.
4. Zhu, P.; Burney, J.; Chang, J.; Jin, Z.; Mueller, N.D.; Xin, Q.; Xu, J.; Yu, L.; Makowski, D.; Ciais, P. Warming reduces global agricultural production by decreasing cropping frequency and yields. *Nat. Clim. Chang.* **2022**, *12*, 1016–1023. [\[CrossRef\]](#)
5. IPCC. *Climate Change 2014: Impacts, Adaptation, and Vulnerability. Part B: Regional Aspects*; Cambridge University Press: Cambridge, UK; New York, NY, USA, 2014.
6. Amede, T.; Konde, A.A.; Muhinda, J.J.; Bigirwa, G. Sustainable Farming in Practice: Building Resilient and Profitable Smallholder Agricultural Systems in Sub-Saharan Africa. *Sustainability* **2023**, *15*, 5731. [\[CrossRef\]](#)
7. Adhikari, U.; Nejadhashemi, A.P.; Woznicki, S.A. Climate change and eastern Africa: A review of impact on major crops. *Food Energy Secur.* **2015**, *4*, 110–132. [\[CrossRef\]](#)
8. Beyene, S.D. The impact of food insecurity on health outcomes: Empirical evidence from sub-Saharan African countries. *BMC Public Health* **2023**, *23*, 338. [\[CrossRef\]](#) [\[PubMed\]](#)
9. FAO. *The State of Food Insecurity in the World (SOFI)*; Food and Agricultural Organization (FAO) of the United Nations and World Bank: Rome, Italy, 2014.
10. FAO. *World Agriculture towards 2015/2030: An FAO Perspective*; FAO: Rome, Italy, 2003; p. 432.
11. Bjornlund, V.; Bjornlund, H.; van Rooyen, A. Why food insecurity persists in sub-Saharan Africa: A review of existing evidence. *Food Secur.* **2022**, *14*, 845–864. [\[CrossRef\]](#)
12. Edmonds, D.E.; Abreu, S.L.; West, A.; Caasi, D.R.; Conley, T.O.; Daft, M.C.; Desta, B.; England, B.B.; Farris, C.D.; Nobles, T.J. Cereal nitrogen use efficiency in sub-Saharan Africa. *J. Plant Nutr.* **2009**, *32*, 2107–2122. [\[CrossRef\]](#)
13. van Ittersum, M.K.; van Bussel, L.G.J.; Wolf, J.; Grassini, P.; van Wart, J.; Guilpart, N.; Claessens, L.; de Groot, H.; Wiebe, K.; Mason-D’Croz, D.; et al. Can sub-Saharan Africa feed itself? *Proc. Natl. Acad. Sci. USA* **2016**, *113*, 14964–14969. [\[CrossRef\]](#)
14. Rezaei, E.E.; Webber, H.; Asseng, S.; Boote, K.; Durand, J.L.; Ewert, F.; Martre, P.; MacCarthy, D.S. Climate change impacts on crop yields. *Nat. Rev. Earth Environ.* **2023**, *4*, 831–846. [\[CrossRef\]](#)
15. Lesk, C.; Anderson, W.; Rigden, A.; Coast, O.; Jägermeyr, J.; McDermid, S.; Davis, K.F.; Konar, M. Compound heat and moisture extreme impacts on global crop yields under climate change. *Nat. Rev. Earth Environ.* **2022**, *3*, 872–889. [\[CrossRef\]](#)
16. Zhao, J.; Yang, X.; Dai, S.; Lv, S.; Wang, J. Increased utilization of lengthening growing season and warming temperatures by adjusting sowing dates and cultivar selection for spring maize in Northeast China. *Eur. J. Agron.* **2015**, *67*, 12–19. [\[CrossRef\]](#)

17. Liu, Z.; Hubbard, K.G.; Lin, X.; Yang, X. Negative effects of climate warming on maize yield are reversed by the changing of sowing date and cultivar selection in Northeast China. *Glob. Chang. Biol.* **2013**, *19*, 3481–3492. [[CrossRef](#)]
18. Troy, T.J.; Kipgen, C.; Pal, I. The impacts of climate extremes and irrigation on US crop yields. *Environ. Res. Lett.* **2015**, *10*, 054013. [[CrossRef](#)]
19. Kheir, A.M.S.; Ammar, K.A.; Attia, A.; Elnashar, A.; Ahmad, S.; El-Gioushy, S.F.; Ahmed, M. Cereal Crop Modeling for Food and Nutrition Security. In *Global Agricultural Production: Resilience to Climate Change*; Ahmed, M., Ed.; Springer International Publishing: Cham, Switzerland, 2022; pp. 183–195.
20. Abera, K.; Crespo, O.; Seid, J.; Mequanent, F. Simulating the impact of climate change on maize production in Ethiopia, East Africa. *Environ. Syst. Res.* **2018**, *7*, 4. [[CrossRef](#)]
21. Basso, B.; Cammarano, D.; Carfagna, E. *Review of Crop Yield Forecasting Methods and Early Warning Systems. GS SAC—Improving Methods for Crops Estimates*; FAO Publication: Rome, Italy, 2013.
22. Baffour-Ata, F.; Tabi, J.S.; Sangber-Dery, A.; Etu-Mantey, E.E.; Asamoah, D.K. Effect of rainfall and temperature variability on maize yield in the Asante Akim North District, Ghana. *Curr. Res. Environ. Sustain.* **2023**, *5*, 100222. [[CrossRef](#)]
23. Kamara, A.Y.; Oyinbo, O.; Manda, J.; Kamara, A.; Idowu, E.O.; Mbavai, J.J. Beyond average: Are the yield and income impacts of adopting drought-tolerant maize varieties heterogeneous? *Clim. Dev.* **2024**, *16*, 67–76. [[CrossRef](#)]
24. Kogo, B.K.; Kumar, L.; Koech, R. Climate change and variability in Kenya: A review of impacts on agriculture and food security. *Environ. Dev. Sustain.* **2021**, *23*, 23–43. [[CrossRef](#)]
25. Abate, T.; Shiferaw, B.; Menkir, A.; Wegary, D.; Kebede, Y.; Tesfaye, K.; Kassie, M.; Bogale, G.; Tadesse, B.; Keno, T. Factors that transformed maize productivity in Ethiopia. *Food Secur.* **2015**, *7*, 965–981. [[CrossRef](#)]
26. Tadesse, T.; Senay, G.B.; Berhan, G.; Regassa, T.; Beyene, S. Evaluating a satellite-based seasonal evapotranspiration product and identifying its relationship with other satellite-derived products and crop yield: A case study for Ethiopia. *Int. J. Appl. Earth Obs. Geoinf.* **2015**, *40*, 39–54. [[CrossRef](#)]
27. Mozny, M.; Tnka, M.; Zalud, Z.; Hlavinka, P.; Nekovar, J.; Potop, V.; Virag, M. Use of a soil moisture network for drought monitoring in the Czech Republic. *Theor. Appl. Climatol.* **2012**, *107*, 88–111. [[CrossRef](#)]
28. Adeyeri, O.E.; Laux, P.; Lawin, A.E.; Ige, S.O.; Kunstmann, H. Analysis of hydrometeorological variables over the transboundary Komadugu-Yobe basin, West Africa. *J. Water Clim. Chang.* **2020**, *11*, 1339–1354. [[CrossRef](#)]
29. Noonni, I.K.; Hagan, D.F.T.; Wang, G.; Ullah, W.; Li, S.; Lu, J.; Bhatti, A.S.; Shi, X.; Lou, D.; Prempeh, N.A.; et al. Spatiotemporal Characteristics and Trend Analysis of Two Evapotranspiration-Based Drought Products and Their Mechanisms in Sub-Saharan Africa. *Remote Sens.* **2021**, *13*, 533. [[CrossRef](#)]
30. Gebrechorkos, S.H.; Hülsmann, S.; Bernhofer, C. Changes in temperature and precipitation extremes in Ethiopia, Kenya, and Tanzania. *Int. J. Climatol.* **2019**, *39*, 18–30. [[CrossRef](#)]
31. Jimenez-Munoz, J.C.; Sobrino, J.A.; Matter, C. Has the Northern Hemisphere been warming or cooling during boreal winter of the last few decades. *Glob. Planet. Chang.* **2013**, *106*, 31–38. [[CrossRef](#)]
32. Farooq, M.; Hussain, M.; Wakeel, A.; Siddique, K.H.M. Salt stress in maize: Effects, resistance mechanisms, and management. A review. *Agron. Sustain. Dev.* **2015**, *35*, 461–481. [[CrossRef](#)]
33. Girma, Y.; Kuma, B.; Bedemo, A. Risk Aversion and Perception of Farmers about Endogenous Risks: An Empirical Study for Maize Producers in Awi Zone, Amhara Region of Ethiopia. *J. Risk Financ. Manag.* **2023**, *16*, 87. [[CrossRef](#)]
34. Higginbottom, T.P.; Adhikari, R.; Foster, T. Rapid expansion of irrigated agriculture in the Senegal River Valley following the 2008 food price crisis. *Environ. Res. Lett.* **2023**, *18*, 014037. [[CrossRef](#)]
35. Diasso, U.; Abiodun, B.J. Drought modes in West Africa and how well CORDEX RCMs simulate them. *Theor. Appl. Climatol.* **2017**, *128*, 223–240. [[CrossRef](#)]
36. Biradar, C.M.; Thenkabail, P.S.; Noojipady, P.; Li, Y.; Dheeravath, V.; Turrall, H.; Velpuri, M.; Gumma, M.K.; Gangalakunta, O.R.P.; Cai, X.L.; et al. A global map of rainfed cropland areas (GMRCA) at the end of last millennium using remote sensing. *Int. J. Appl. Earth Obs. Geoinf.* **2009**, *11*, 114–129. [[CrossRef](#)]
37. Adeyeri, O.E.; Ishola, K.A. Variability and trends of actual evapotranspiration over West Africa: The role of environmental drivers. *Agric. For. Meteorol.* **2021**, *308*, 108574. [[CrossRef](#)]
38. Beck, H.E.; Zimmermann, N.E.; McVicar, T.R.; Vergopolan, N.; Berg, A.; Wood, E.F. Present and future Köppen-Geiger climate classification maps at 1-km resolution. *Sci. Data* **2018**, *5*, 180214. [[CrossRef](#)]
39. National Aeronautics and Space Administration. National Aeronautics and Space Administration (NASA) Shuttle Radar Topography Mission (SRTM) Home Page. Available online: <https://lpdaac.usgs.gov/products/srtmg11v003/> (accessed on 10 December 2023).
40. ESACCI. European Space Agency Climate Change Initiative (ESACCI) Land Use Land Cover (LULC) Map. Available online: <https://www.esa-landcover-cci.org/> (accessed on 10 December 2023).
41. Chen, M.; Shi, W.; Xie, P.; Silva, V.B.S.; Kousky, V.E.; Wayne Higgins, R.; Janowiak, J.E. Assessing objective techniques for gauge-based analyses of global daily precipitation. *J. Geophys. Res. Atmos.* **2008**, *113*, D04110. [[CrossRef](#)]
42. Xie, P.; Yatagai, A.; Chen, M.; Hayasaka, T.; Fukushima, Y.; Liu, C.; Yang, S. A Gauge-Based Analysis of Daily Precipitation over East Asia. *J. Hydrometeorol.* **2007**, *8*, 607–626. [[CrossRef](#)]

43. National Oceanic and Atmospheric Administration (NOAA). Homepage. Available online: <ftp://ftp.cdc.noaa.gov/Datasets> (accessed on 23 December 2023).
44. Global Land Evaporation Amsterdam Model (GLEAM). Homepaage. Available online: www.GLEAM.eu (accessed on 10 December 2023).
45. Martens, B.; Miralles, D.G.; Lievens, H.; van der Schalie, R.; de Jeu, R.A.M.; Fernández-Prieto, D.; Beck, H.E.; Dorigo, W.A.; Verhoest, N.E.C. GLEAM v3: Satellite-based land evaporation and root-zone soil moisture. *Geosci. Model Dev.* **2017**, *10*, 1903–1925. [[CrossRef](#)]
46. Miralles, D.G.; De Jeu, R.A.M.; Gash, J.H.; Holmes, T.R.H.; Dolman, A.J. Magnitude and variability of land evaporation and its components at the global scale. *Hydrol. Earth Syst. Sci.* **2011**, *15*, 967–981. [[CrossRef](#)]
47. Miralles, D.G.; Holmes, T.R.H.; De Jeu, R.A.M.; Gash, J.H.; Meesters, A.G.C.A.; Dolman, A.J. Global land-surface evaporation estimated from satellite-based observations. *Hydrol. Earth Syst. Sci.* **2011**, *15*, 453–469. [[CrossRef](#)]
48. US Department of Agriculture. Homepage. Available online: <https://www.indexmundi.com/agriculture/> (accessed on 5 January 2024).
49. Schulzweida. CDO User Guide (Version 2.0.0). 2021. Available online: <https://zenodo.org/records/5614769> (accessed on 29 March 2024).
50. Mann, H.B. Nonparametric Tests Against Trend. *Econometrica* **1945**, *13*, 245–259. [[CrossRef](#)]
51. Sen, P.K. Estimates of the Regression Coefficient Based on Kendall’s Tau. *J. Am. Stat. Assoc.* **1968**, *63*, 1379–1389. [[CrossRef](#)]
52. Nooni, I.K.; Ogou, F.K.; Lu, J.; Nakoty, F.M.; Chaibou, A.A.; Habtemicheal, B.A.; Sarpong, L.; Jin, Z. Temporal and Spatial Variations of Potential and Actual Evapotranspiration and the Driving Mechanism over Equatorial Africa Using Satellite and Reanalysis-Based Observation. *Remote Sens.* **2023**, *15*, 3201. [[CrossRef](#)]
53. Li, X.; Takahashi, T.; Suzuki, N.; Kaiser, H.M. The impact of climate change on maize yields in the United States and China. *Agric. Syst.* **2011**, *104*, 348–353. [[CrossRef](#)]
54. Niu, X.-K.; Xie, R.-Z.; Liu, X.; Zhang, F.-L.; Li, S.-K.; Gao, S.-J. Maize Yield Gains in Northeast China in the Last Six Decades. *J. Integr. Agric.* **2013**, *12*, 630–637. [[CrossRef](#)]
55. Wang, T.; Li, N.; Li, Y.; Lin, H.; Yao, N.; Chen, X.; Li Liu, D.; Yu, Q.; Feng, H. Impact of climate variability on grain yields of spring and summer maize. *Comput. Electron. Agric.* **2022**, *199*, 107101. [[CrossRef](#)]
56. USAID. *Agricultural Adaptation to Climate Change in the Sahel*; U.S. Agency for International Development: Washington, DC, USA, 2014.
57. FAO. *Water and Soil Requirements*; Food and Agriculture Organisation: Rome, Italy, 1991.
58. Palmer, P.I.; Wainwright, C.M.; Dong, B.; Maidment, R.I.; Wheeler, K.G.; Gedney, N.; Hickman, J.E.; Madani, N.; Folwell, S.S.; Abdo, G.; et al. Drivers and impacts of Eastern African rainfall variability. *Nat. Rev. Earth Environ.* **2023**, *4*, 254–270. [[CrossRef](#)]
59. Liu, Y.; Liu, Y.; Wang, W.; Fan, X.; Cui, W. Soil moisture droughts in East Africa: Spatiotemporal patterns and climate drivers. *J. Hydrol. Reg. Stud.* **2022**, *40*, 101013. [[CrossRef](#)]
60. Myeni, L.; Moeletsi, M.E.; Clulow, A.D. Present status of soil moisture estimation over the African continent. *J. Hydrol. Reg. Stud.* **2019**, *21*, 14–24. [[CrossRef](#)]
61. Yuan, Z.; NourEldeen, N.; Mao, K.; Qin, Z.; Xu, T. Spatiotemporal Change Analysis of Soil Moisture Based on Downscaling Technology in Africa. *Water* **2022**, *14*, 74. [[CrossRef](#)]
62. Nooni, I.K.; Wang, G.; Hagan, D.F.T.; Lu, J.; Ullah, W.; Li, S. Evapotranspiration and its Components in the Nile River Basin Based on Long-Term Satellite Assimilation Product. *Water* **2019**, *11*, 1400. [[CrossRef](#)]
63. Camberlin, P. Temperature trends and variability in the Greater Horn of Africa: Interactions with precipitation. *Clim. Dyn.* **2017**, *48*, 477–498. [[CrossRef](#)]
64. Nicholson, S.E.; Nash, D.J.; Chase, B.M.; Grab, S.W.; Shanahan, T.M.; Verschuren, D.; Asrat, A.; Lézine, A.-M.; Umer, M. Temperature variability over Africa during the last 2000 years. *Holocene* **2013**, *23*, 1085–1094. [[CrossRef](#)]
65. Brenya, R.; Zhu, J. Agricultural extension and food security—The case of Uganda. *Glob. Food Secur.* **2023**, *36*, 100678. [[CrossRef](#)]
66. Kebede, D.; Emanu, B.; Tesfay, G. Impact of land acquisition for large-scale agricultural investments on food security status of displaced households: The case of Ethiopia. *Land Use Policy* **2023**, *126*, 106507. [[CrossRef](#)]
67. Kirui, O.K.; Kornher, L.; Bekchanov, M. Productivity growth and the role of mechanisation in African agriculture. *Agrekon* **2023**, *62*, 80–97. [[CrossRef](#)]
68. De Groote, H.; Omondi, L.B. Varietal turn-over and their effect on yield and food security—Evidence from 20 years of household surveys in Kenya. *Glob. Food Secur.* **2023**, *36*, 100676. [[CrossRef](#)] [[PubMed](#)]
69. Jensen, M.E. *Water Consumption by Agricultural Plants*; Academic Press: New York, NY, USA, 1968; pp. 1–22.
70. Li, Z.; Yang, P.; Tang, H.; Wu, W.; Yin, H.; Liu, Z.; Zhang, L. Response of maize phenology to climate warming in Northeast China between 1990 and 2012. *Reg. Environ. Chang.* **2014**, *14*, 39–48. [[CrossRef](#)]
71. Lobell, D.B. Changes in diurnal temperature range and national cereal yields. *Agric. For. Meteorol.* **2007**, *145*, 229–238. [[CrossRef](#)]
72. Zhang, Z.; Wei, J.; Li, J.; Jia, Y.; Wang, W.; Li, J.; Lei, Z.; Gao, M. The impact of climate change on maize production: Empirical findings and implications for sustainable agricultural development. *Front. Environ. Sci.* **2022**, *10*, 954940. [[CrossRef](#)]
73. Simanjuntak, C.; Gaiser, T.; Ahrends, H.E.; Ceglar, A.; Singh, M.; Ewert, F.; Srivastava, A.K. Impact of climate extreme events and their causality on maize yield in South Africa. *Sci. Rep.* **2023**, *13*, 12462. [[CrossRef](#)]

-
74. Schlenker, W.; Lobell, D.B. Robust negative impacts of climate change on African agriculture. *Environ. Res. Lett.* **2010**, *5*, 014010. [[CrossRef](#)]
 75. Olasehinde, T.S.; Qiao, F.; Mao, S. Impact of Improved Maize Varieties on Production Efficiency in Nigeria: Separating Technology from Managerial Gaps. *Agriculture* **2023**, *13*, 611. [[CrossRef](#)]

Disclaimer/Publisher's Note: The statements, opinions and data contained in all publications are solely those of the individual author(s) and contributor(s) and not of MDPI and/or the editor(s). MDPI and/or the editor(s) disclaim responsibility for any injury to people or property resulting from any ideas, methods, instructions or products referred to in the content.